Revised M06-L functional for improved accuracy on chemical reaction barrier heights, noncovalent interactions, and solid-state physics

Ying Wang[a], Xinsheng Jin[a], Haoyu S. Yu[b,c,d], Donald G. Truhlar[b,c,d,1], and Xiao He[a,e,1]

[a]School of Chemistry and Molecular Engineering, State Key Laboratory of Precision Spectroscopy, East China Normal University, Shanghai 200062, China; [b]Chemical Theory Center, Department of Chemistry, University of Minnesota, Minneapolis, MN 55455-043; [c]Nanoporous Materials Genome Center, Department of Chemistry, University of Minnesota, Minneapolis, MN 55455-043; [d]Minnesota Supercomputing Institute, University of Minnesota, Minneapolis, MN 55455-0431; and [e]New York University–East China Normal University (NYU–ECNU) Center for Computational Chemistry, NYU Shanghai, Shanghai 200062, China

Contributed by Donald G. Truhlar, June 29, 2017 (sent for review April 5, 2017; reviewed by Gregory A. Voth and Weitao Yang)

We present the revM06-L functional, which we designed by optimizing against a larger database than had been used for Minnesota 2006 local functional (M06-L) and by using smoothness restraints. The optimization strategy reduced the number of parameters from 34 to 31 because we removed some large terms that increased the required size of the quadrature grid and the number of self-consistent-field iterations. The mean unsigned error (MUE) of revM06-L on 422 chemical energies is 3.07 kcal/mol, which is improved from 3.57 kcal/mol calculated by M06-L. The MUE of revM06-L for the chemical reaction barrier height database (BH76) is 1.98 kcal/mol, which is improved by more than a factor of 2 with respect to the M06-L functional. The revM06-L functional gives the best result among local functionals tested for the noncovalent interaction database (NC51), with an MUE of only 0.36 kcal/mol, and the MUE of revM06-L for the solid-state lattice constant database (LC17) is half that for M06-L. The revM06-L functional also yields smoother potential curves, and it predicts more-accurate results than M06-L for seven out of eight diversified test sets not used for parameterization. We conclude that the revM06-L functional is well suited for a broad range of applications in chemistry and condensed-matter physics.

Kohn–Sham density functional theory | molecular thermochemistry | solid-state physics | chemical energetics | chemical structures

Over the past 30 years, Kohn–Sham density functional theory (KS-DFT) has become the most robust and popular electronic structure method for chemistry and condensed-matter physics. However, the accuracy of KS-DFT depends on the quality of the exchange–correlation functional, and an exact functional is unknown (1). Much effort has been devoted to the development of better approximations to the exchange–correlation functional. Useful functionals should be accurate and economical to use, because the high performance-to-cost ratio is the leading driver of the widespread use of KS-DFT. Particularly well positioned on the performance-to-cost scale are functionals that depend only on local properties, which are called local functionals, especially by chemists (they are also called "semilocal," especially by physicists; here we use "local"). Local density functionals usually depend on local spin densities $[\rho_\sigma(\mathbf{r}), \sigma = \alpha, \beta$, where $\mathbf{r}$ is a point in real space] and their gradients ($|\nabla\rho_\sigma|$) and sometimes also on the spin-specific kinetic energy density $\tau_\sigma(\mathbf{r})$, which, in atomic units, is given by $(1/2)\sum_{i=1}^{n_\sigma}|\nabla\psi_{i\sigma}(\mathbf{r})|^2$, where $\psi_{i\sigma}$ is the spatial part of an occupied Kohn–Sham spin orbital, and n_σ is the number of occupied spin orbitals of spin σ. Local functionals do not include nonlocal Hartree–Fock exchange energy or nonlocal correlation energy.

An exact density functional cannot be an explicit and differentiable functional of the density, local or nonlocal (2), but local approximations are still preferred for a wide variety of applications (3–6), and they have been widely used in both chemistry and solid-state physics. A main reason is that local functionals require less computational cost than nonlocal functionals (7–11) in plane wave codes and for large molecules when density-fitting algorithms are used (12–14) in Gaussian basis function codes; thus they are more suitable for practical computations on simulations of complex systems, macromolecules, and condensed-phase systems treated with periodic boundary conditions. In addition, local functionals are usually more accurate for systems containing transition metals (TMs) where density-based exchange functionals can describe the static correlation better than Hartree–Fock exchange (15, 16). Thirdly, local functionals often provide more-accurate bond lengths and vibrational frequencies for molecules at equilibrium geometries than do functionals that contain Hartree–Fock exchange, which are called hybrid functionals (17, 18).

The Minnesota 2006 local functional (M06-L) (19), which was published in 2006, is a local meta-generalized gradient approximation (meta-GGA, where meta denotes dependence on τ_σ) that was parameterized against several molecular databases. M06-L has broad accuracy for main-group thermochemistry, thermochemical kinetics, metallochemical and noncovalent interactions, bond lengths, and vibrational frequencies; for example, it has been found to perform well in a variety of tests against accurate and experimental data. However, M06-L still has room for improvement in terms of overall accuracy, numerical stability, required fineness of integration grids, and self-consistent field (SCF) convergence. For

Significance

Local exchange–correlation functionals, which depend on the local spin densities, their gradients, and the local spin-specific kinetic energy densities, have been widely used for electronic structure calculations in both chemistry and physics, owing to their computational efficiency in plane wave codes and for large molecules and to their relatively high accuracy for transition metals and other inherently multiconfigurational systems. Minnesota 2006 local functional (M06-L) has proven to be one of the most accurate local functionals currently available, but it has room for improvement with regard to numerical stability and overall accuracy. Here we present a revised M06-L functional, named revM06-L, which gives both smoother potential energy curves and improved overall accuracy, especially for chemical reaction barrier heights, noncovalent interactions, and solid-state physics.

Author contributions: H.S.Y., D.G.T., and X.H. designed research; Y.W., X.J., and X.H. performed research; Y.W., X.J., H.S.Y., D.G.T., and X.H. analyzed data; and Y.W., X.J., H.S.Y., D.G.T., and X.H. wrote the paper.

Reviewers: G.A.V., The University of Chicago; and W.Y., Duke University.

The authors declare no conflict of interest.

[1]To whom correspondence may be addressed. Email: xiaohe@phy.ecnu.edu.cn or truhlar@umn.edu.

This article contains supporting information online at www.pnas.org/lookup/suppl/doi:10.1073/pnas.1705670114/-/DCSupplemental.

Table 1. MUE (kcal/mol) for the AME422 database and its subdatabases

Functional	MGBE137*	TMBE33†	BH76‡	NC51§	EE18¶	AME422#
Local						
MN15-L	1.58	5.16	1.66	0.45	3.71	2.32
revM06-L	2.01	6.72	1.98	0.36	7.50	3.07
M06-L	2.37	5.46	3.98	0.42	7.71	3.57
GAM	2.65	6.24	5.25	0.77	6.93	4.56
τ-HCTH	2.80	7.83	6.39	0.84	14.02	5.42
TPSS	2.79	8.36	8.31	0.89	7.58	5.47
VSXC	2.45	7.77	4.91	1.68	7.63	6.13
PBE	4.94	10.88	8.87	0.88	7.69	7.85
Nonlocal						
MN15	1.32	5.54	1.36	0.20	6.28	2.24
M06	1.86	7.60	2.16	0.35	8.45	2.84
B97-1	1.90	5.26	3.89	0.53	7.31	3.20
M06-2X	1.91	19.11	1.18	0.23	7.86	3.35
ωB97X-D	2.30	8.70	3.05	0.30	8.30	3.38
M08-HX	2.88	17.59	0.97	0.25	5.78	3.57
B3LYP	3.07	7.32	4.39	0.81	6.58	4.80
PBE0	2.69	10.18	3.83	0.55	6.85	5.22

*The MGBE137 database consists of SR-MGM-BE9, SR-MGN-BE107, MR-MGM-BE4, and MR-MGN-BE17.
†The TMBE33 database consists of SR-TM-BE17, MR-TM-BE13, and MR-TMD-BE3.
‡The BH76 database consists of HTBH38/08 and NHTBH38/08.
§The NC51 database consists of NGDWI21 and NCCE30.
¶The EE18 database consists of 3dEE8, 4dAEE5, and pEE5.
#The AME422 database consists all of the 25 subdatabases.

instance, the mean unsigned error (MUE) of M06-L for the BH76 chemical reaction barrier height database is 4.0 kcal/mol, which is significantly larger than more-recent local functionals, such as Minnesota 2011 local functional (M11-L) (20), Minnesota nonseparable 2012 local functional (MN12-L) (21), and Minnesota nonseparable 2015 local functional (MN15-L) (17). In addition, M06-L sometimes lacks computational stability and requires finer grid sizes for convergence (22, 23).

Like other functionals, M06-L is not uniformly accurate for various types of interactions. Especially noteworthy is that the lattice constants of solids predicted by M06-L have larger errors than those obtained by several other local functionals, such as local density approximation, revised Tao–Perdew–Staroverov–Scuseria functional (revTPSS) (24), and meta-GGA made simple 2 (MGGA_MS2) (25).

In this work, to achieve higher across-the-board accuracy and to improve the accuracy for chemical reaction barrier heights, noncovalent interactions, and lattice constants, we reparameterized the M06-L functional by fitting to a larger database including both molecular and solid-state data. The resulting functional is named revM06-L. Furthermore, similar to the previous gradient approximation for molecules (GAM) (26), MN15-L (17), and Minnesota nonseparable 2015 functional (MN15) (18), smoothness restraints on the fitting parameters were used during fitting procedure. We also removed some large electronic integral terms in the functional, which requires finer quadrature grid size to converge the energy. By introducing the smoothness restraints and removing the large integral terms, we were able to make the revM06-L functional less sensitive to the size of quadrature grid and require a smaller number of SCF iterations.

Results and Discussion

All parameters were optimized in a self-consistent fashion, and full details of the functionals and their optimization are provided in *SI Appendix*. All calculations were carried out using a locally modified version (27) of the *Gaussian 09* (28) program. Minnesota Database 2015A (17, 26) was used as the training dataset, as summarized in *SI Appendix*, Table S1. *SI Appendix*, Table S2 gives the values of the linear parameters of the final revM06-L functional. We find that, as a result of the smoothness restraints that were added in the optimization, the parameters in revM06-L are much smaller than those in M06-L. In addition, as mentioned in the Introduction, we also removed some large terms. As a result, the total number of parameters in revM06-L is reduced to 31, compared with 34 parameters in the original M06-L functional. The final functional form has 32 terms.

In this work, in addition to comparing the results of revM06-L with those of the original M06-L (19) functional, we also selected some other functionals for comparison. In previous work (17, 18, 26), we calculated the entire database of 422 atomic and molecular energies (AME422) with a large number of density functionals. Here, based on those evaluations, we chose for comparison the functional of each type [gradient approximation (GA), meta-GA, hybrid GA, and hybrid meta-GA] that gives the lowest MUE for AME422. The functionals thus selected in each category are GAM (26) in GAs, MN15-L (17) in meta-GAs, Becke 1997 revision-1 functional (B97-1) (29) in hybrid GAs, and MN15 (18) in hybrid meta-GAs. (Note that a GA may be either a GGA or a nonseparable GA.) We also selected one of the most popular functionals in each of these four categories, namely, Perdew–Burke–Ernzerhof functional (PBE) (30) in GAs, TPSS (31) in meta-GAs, Becke 3-parameter Lee–Yang–Parr functional (B3LYP) (32–34) in hybrid GAs, and Minnesota 2006 with-double-Hartree–Fock-exchange functional (M06-2X) (14) in hybrid meta-GAs. In addition, in Table 1, we also compare the results to those of some other functionals chosen as representative of other approaches, in particular Van Voorhis–Scuseria exchange-correlation functional (VSXC) (35) and meta Hamprecht–Cohen–Tozer–Handy functional (τ-HCTH) (36) as meta-GGAs, range-separated Becke 1997 functional with nonzero Hartree–Fock exchange for all interelectronic distances and with molecular mechanics dispersion (ωB97X-D) (37) as a range-separated hybrid GGA with molecular mechanics damped dispersion, and Minnesota 2006 functional (M06) (14) and Minnesota 2008 high-Hartree–Fock-exchange functional (M08-HX) (38) as hybrid meta-GGAs. In a few of the comparisons of results for the nontraining test sets, we also compare with results for a few other functionals.

Atomic and Molecular Energies. Table 1 shows the performance for the full set of atomic and molecular energies in the last column, and for selected interesting subsets in earlier columns, in particular

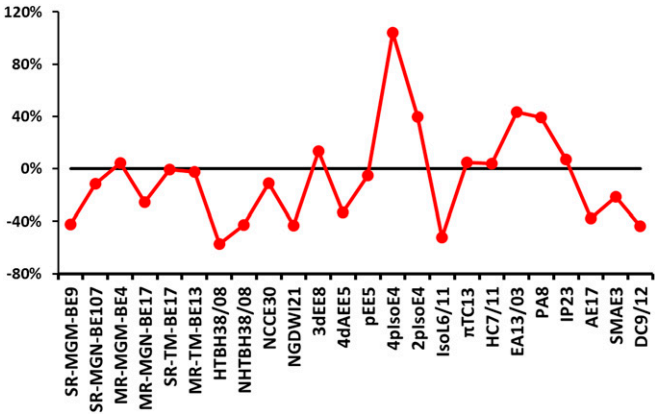

Fig. 1. The percentage change in MUEs of revM06-L relative to M06-L on atomic and molecular energetic databases (subdatabases of AME22). The ordinate is [MUE(revM06-L)–MUE(M06-L)]/MUE(M06-L). The MR-TMD-BE3 subdatabase is not included in the figure.

Table 2. MUEs for lattice constants (LC17: nearest-neighbor distances in angstroms) and semiconductor band gaps (SBG31 in electron volts)

Functional	Type	LC17	SBG31
HSE06	RS-hybrid GGA	0.041	0.26
revM06-L	Meta-GGA	0.041	0.45
MN15-L	Meta-NGA	0.046	0.80
TPSS	Meta-GGA	0.055	0.85
M06-L	Meta-GGA	0.080	0.73
PBE	GGA	0.068	0.98
VSXC	Meta-GGA	0.078	0.97
GAM	NGA	0.092	0.99
τ-HCTH	Meta-GGA	0.107	0.92
MN15	Hybrid meta-NGA	NA	0.92

for 137 main-group bond energies (MGBE137), 33 TM bond energies (TMBE33), 76 reaction barrier heights (BH76), 51 noncovalent interaction energies (NC51), and 18 p-block and transition metal excitation energies (EE18).

Table 1 shows that the revM06-L functional gives better results than M06-L for MGBE137, BH76, NC51, EE18, and AME422, and it gives the fourth best results overall among the 16 local and nonlocal functionals listed in Table 1, with an MUE of 3.1 kcal/mol. The three best-performing functionals in Table 1 for AME422 are MN15, MN15-L, and M06, with MUEs of 2.2 kcal/mol to 2.8 kcal/mol.

The performance of revM06-L on barrier heights (BH76) is significantly improved compared with M06-L, decreasing the MUE from 4.0 kcal/mol to 2.0 kcal/mol. For barrier heights, revM06-L trails only one local functional, MN15-L, and it also outperforms five hybrid functionals shown in Table 1. Most density functionals (with MN15 being the prime exception) do not give accurate results for both barrier heights and TM bond energies. For example, the two functionals in Table 1 with the best results for BH76, M08-HX and M06-2X, predict the worst results for TMBE33. Only MN15-L, MN15, and revM06-L have an MUE below 7.0 kcal/mol for TMBE33 and below 2.0 kcal/mol for BH76.

It is difficult to predict weak noncovalent interactions accurately by local density functionals (39) without nonlocal electron correlation (40, 41) or empirical van der Waals corrections (42). Nevertheless, the functional form designed for M06-type functionals enables them to describe weak noncovalent interactions at van der Waals geometries, where the electron densities of the interacting partners overlap. Table 1 shows that, among local functionals, revM06-L gives the lowest MUE for noncovalent interactions (NC51).

Furthermore, Table 1 shows that revM06-L gives the second-lowest MUE for MGBE137 among local functionals, and it gives better results for EE18 than M06-L.

Fig. 1 and *SI Appendix*, Table S5 show a detailed comparison of MUEs for all 25 atomic and molecular energy (AME) subdatabases between M06-L and revM06-L. The revM06-L functional gives a lower MUE for 15 of the 25 subdatabases, and, in 12 of these 15 cases, the difference is more than 10%. In particular, the performances on three subdatabases of main-group bond energies (SR-MGM-BE9, SR-MGN-BE107, and MR-MGN-BE17) and two subdatabases of TM bond energies (SR-TM-BE17 and MR-TM-BE13) are all improved. However, the accuracy on MR-TMD-BE3 becomes worse. Notably, the MUEs of revM06-L for HTBH38/08, NHTBH38/08, NGDWI21, 4dAEE5, IsoL6/11, AE17, and DC9/12 are all 30 to 60% lower than those of M06-L.

Molecular Structure Database. *SI Appendix*, Table S6 shows the performance of revM06-L on the molecular structure database (MS10), including six diatomic bond lengths of light-atom molecules (DGL6) and four diatomic bond lengths of molecules with Zn, Br, or Ag (DGH4). The revM06-L functional gives the second-best result (MUE = 0.009 Å) for DGH4, trailing only MN15, which has an MUE of 0.008 Å vs. 0.011 Å for M06-L. The revM06-L functional gives the fourth-lowest MUE of 0.009 Å for the full MS10 among 22 functionals in *SI Appendix*, Table S6, with MN15, MN15-L, and PBE0 being the top three with MUEs of 0.006, 0.008, and 0.008 Å, respectively. We conclude that the revM06-L functional can provide good bond lengths for molecular structures.

Solid-State Databases. Table 2 shows the MUEs of 16 functionals [representative local functionals and HSE06 (43), which is a screened-exchange hybrid-GGA] on two solid-state databases: 17 lattice constants (LC17, a training set) and 31 semiconductor band gaps (SBG31, a nontraining test set). These calculations were carried out with periodic boundary conditions as discussed in previous work (15, 17, 18, 44). Table 2 shows that the MUE of revM06-L for LC17 is reduced to 0.041 Å from 0.080 Å for M06-L, and the MUE for SBG31 is reduced to 0.45 eV from 0.73 eV. The new revM06-L gives the best results among all local functionals in Table 2 for both LC17 and SBG31. Therefore, the revM06-L functional has the across-the-board accuracy for both chemistry and physics databases adopted in this work.

Performance of revM06-L on Nontraining Test Sets. The revM06-L functional has been tested against nontraining databases (see *SI Appendix*, Table S3), including semiconductor band gaps (SBG31), noncovalently bound complexes (S66 and S66x8), vertical excitation energies (EE69), TM coordination reactions (WCCR10), TM reaction barrier heights (TMBH21), TM dimer equilibrium bond lengths (TMDBL7), alkyl bond dissociation energies (ABDE13), and transition state geometries (TSG48). SBG31 was already discussed in *Solid-State Databases*; here we discuss the other seven.

The S66 database (45) has benchmark interaction energies of 66 noncovalent binding complexes at the equilibrium van der Waals geometry, and it can be divided into three subdatabases: damped-dispersion-dominated complexes (DD23), hydrogen-bonded complexes (HB23), and complexes dominated by a mix of damped dispersion and electrostatic interactions (Mix20). The S66x8 database includes the S66 dataset and also contains accurate interaction energies for these 66 complexes at seven other interaction distances; as a result, the S66x8 database has 528 interaction energies. Fig. 2 and *SI Appendix*, Table S8 show the results for 13 functionals for the S66 database, its subdatabases, and the S66x8 database (18, 46). As shown in Fig. 2, the revM06-L functional performs better than M06-L, M06, and MN15-L. The revM06-L gives better results than the other four local functionals

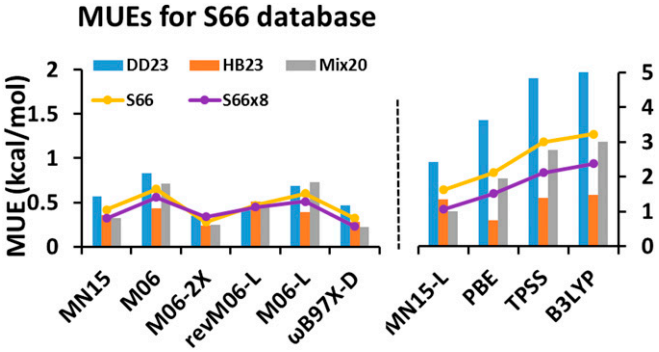

Fig. 2. The MUEs (kilocalories per mole) of 10 selected density functionals for the S66 and S66x8 databases and subdatabases.

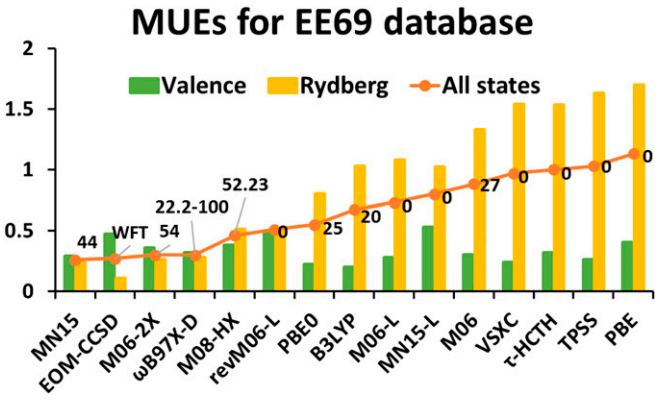

Fig. 3. The MUEs (in electron volts) of 15 selected methods for the vertical excitation energies of 30 valence states and 39 Rydberg states and for all 69 transitions. The numerical labels represent the percentages of Hartree–Fock exchange; when a range is indicated, the first value corresponds to small interelectronic separation, and the second corresponds to large interelectronic separation. WFT, wave function theory.

in *SI Appendix*, Table S8 for DD23, Mix20, S66, and S66x8, although M06-L is better for HB23. The revM06-L functional is better than six of the eight nonlocal functionals in the table for DD23, better than four of them for S66 and S66x8, better than two for Mix20, and better than one for HB23. Note that *SI Appendix*, Table S8 includes PW6B95-D3(BJ) (47, 48), a hybrid meta-GGA with molecular mechanics corrections; this functional is included because it has been emphasized elsewhere (49) that PB6B95 with a D3-type dispersion correction has broad accuracy, and *SI Appendix*, Table S8 bears this out.

Fig. 3 and *SI Appendix*, Table S9 show the results for time-dependent density functional calculation of valence and Rydberg excitation energies of 11 organic molecules (EE69) using various functionals. The data for other functionals were reported in previous studies (50, 51). As shown in Fig. 3, hybrid functionals give the best performance on EE69; the functional that performs best is MN15 with an MUE of 0.26 eV for all states. The revM06-L functional performs approximately equally well for valence and Rydberg excitation energies and reduces the overall MUE of 0.73 eV for M06-L to 0.51 eV so that it gives the best overall performance for EE69 among local functionals; it even outperforms some hybrid functionals, e.g., PBE0 (52), B3LYP, and M06 with MUEs of, respectively, 0.55, 0.67, and 0.88 eV for all states.

Table 3 and *SI Appendix*, Table S10 show the performance of several representative functionals for the transition-metal coordination-complex reaction database (WCCR10). The revM06-L, M06-L, ωB97X (53), and ωB97X-D results are calculated in the present study. The MN15, MN15-L, and GAM results are taken from ref. 18. All other results are taken from ref. 54. Table 3 shows that the revM06-L functional gives the best results for WCCR10 among functionals presented in this table. The MUE of revM06-L is 4.8 kcal/mol, which is improved from 5.2 kcal/mol given by M06-L.

Table 3. MUEs (kilocalories per mole) for ligand dissociation energies of large cationic transition-metal complexes (WCCR10)

Functional	Type	WCCR10
revM06-L	Meta-GGA	**4.81**
MN15	Hybrid meta-NGA	5.04
M06-L	Meta-GGA	**5.24**
MN15-L	Meta-NGA	5.46
PBE0	Hybrid GGA	6.40
GAM	NGA	6.60
ωB97X-D	RS-hybrid GGA+MM*	7.29
PBE	GGA	7.58
TPSS	GGA	7.84
B3LYP	Hybrid GGA	9.30

*MM denotes molecular mechanics dispersion corrections to the SCF energy.

The database of transition-metal reaction barrier heights (TMBH21) involving Mo, W, Zr, and Re (55–57) was tested, and the results are given in *SI Appendix*, Table S11. Although the revM06-L functional performs worse on the reaction barrier heights of molecules containing W and Zr than M06-L, revM06-L still gives lower average MUE for TMBH21 than M06-L, owing to reduced MUEs on reactions with elements Mo and Re. Re data are not involved in the training set, but revM06-L gives the best results for Re among all local functionals and ranks fifth among the 15 functionals presented in *SI Appendix*, Table S11. Moreover, only one local functional, MN15-L, gives lower average MUE for TMBH21 than revM06-L. The good performance of revM06-L for TMBE33 in Table 1 and TMBH21 in *SI Appendix*, Table S11 and the excellent performance for WCCR10 in Table 3 make revM06-L a good choice of functional for TM chemistry.

SI Appendix, Table S12 shows the results of 13 functionals (seven local functionals and six hybrid functionals) for the homonuclear transition-metal dimer bond length database (58) (TMDBL7). The revM06-L functional performs slightly worse than M06-L. However, the results for TMDBL7 given by M06-L and revM06-L are very close, with MUEs of 0.034 and 0.037 Å, respectively. *SI Appendix*, Table S12 shows that local functionals predict more-accurate equilibrium bond lengths than hybrid functionals for TM dimers. The five best-performing functionals for this database are MGGA_MS2 (22, 25), MN15-L, M06-L, revM06-L, and LSDA, with MUEs(2) between 0.028 Å and 0.043 Å, whereas ωB97X-D has an MUE of 0.085 Å.

Thirteen alkyl bond dissociation energies (ABDE13) in the SR-MGN-BE database of Minnesota Database 2015B (18) are also taken as a test set in this study. The results of 21 functionals on ABDE13 are shown in *SI Appendix*, Table S13. The revM06-L functional significantly improves the result for ABDE13 compared with M06-L, lowering the MUE from 5.4 kcal/mol to 2.4 kcal/mol. Furthermore, revM06-L gives the best result among 11 local functionals in *SI Appendix*, Table S13. The MUE of 2.4 kcal/mol is close to the MUE of 2.0 kcal/mol that revM06-L gives for the MGBE137 database in the training set (Table 1 and *SI Appendix*, Table S4). Therefore, the accuracy of the revM06-L functional does transfer well from the training database to a nontraining test set.

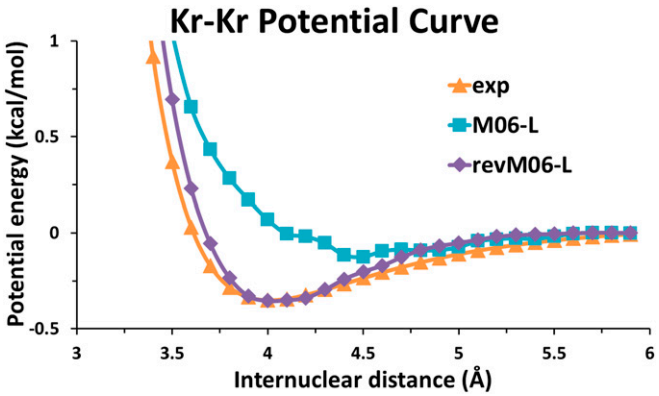

Fig. 4. Kr–Kr potential curve calculated by M06-L and revM06-L with the (99, 590) grid and the aug-cc-pVQZ basis set compared with the experimental curve.

A challenging problem for local functionals is to predict geometries of transition state structures, which are first-order saddle points for chemical reactions. To examine this question, *SI Appendix*, Table S14 shows the results of TSGs in the TSG48 subdatabase (59), which contains 48 TSG data (in particular, internuclear distances in transition state structures) for 16 main-group reactions. As shown in *SI Appendix*, Table S14, hybrid functionals generally predict more-accurate TSGs than local functionals. The revM06-L functional gives better results for TSG48 than does M06-L; the respective MUEs are 0.052 and 0.070 Å. The revM06-L functional also gives a lower MUE than do 14 of the other 17 local functionals in *SI Appendix*, Table S14, with M11-L, MN15-L, and MN12-L being the top three, with MUEs of 0.035 Å to 0.047 Å. The revM06-L functional also outperforms several hybrid functionals, including the widely used B3LYP, which has an MUE of 0.065 Å. Note that no transition-state geometric data were used for optimization of any of the functionals.

Potential Energy Curves of Rare Gas and Water Dimers. The potential curves calculated for rare gas dimers Ar_2 and Kr_2 using revM06-L and M06-L with the aug-cc-pVQZ basis set and a grid having 99 radial shells and 590 angular points per shell for each atom are shown in *SI Appendix*, Fig. S2 and Fig. 4. The calculated curves are also compared with experimental results (60). The figures show that the revM06-L functional provides much more accurate binding curves for Ar_2 and Kr_2 than does M06-L. Although the binding energies of these two dimers near the equilibrium geometries are in the NGDWI21 database of the training set, it is encouraging that the potential curves as functions of internuclear distance are reasonable, although the long-range tail is missing because KS-DFT with a local functional does not predict the long-range dispersion in the region where the interacting charge clouds do not overlap. The M06-L potential curves yield too-shallow minima for these two systems. Moreover, the equilibrium binding distances calculated by M06-L are 0.3 Å to 0.5 Å larger than the experimental ones. In contrast, the revM06-L functional not only gives the accurate binding energy near the equilibrium but also predicts accurate equilibrium distances for both Ar_2 and Kr_2.

The calculated potential curves for Ar_2 and Kr_2 by revM06-L are also much smoother than those obtained with M06-L. It has been reported that the grid errors exhibited by the M06 suite of functionals arise from integration errors in the exchange–correlation component of the energy (23). At least 250 radial shells are required to make the potential curves of rare gas dimers smooth with M06-L (25). As shown in *SI Appendix*, Fig. S2 and Fig. 4, the potential curves of Ar_2 and Kr_2 calculated by the revM06-L functional are already smooth with the (99, 590) grid, because we used smoothness restraints on the fitting parameters and also removed some large electronic integral terms in the functional form. In contrast, the potential curves calculated by M06-L show some oscillations, which may cause computational instability when estimating small energy changes. We conclude that the grid requirements are greatly reduced for the revM06-L functional.

Water dimer potential curves calculated by M06-L, revM06-L, MP2, and CCSD(T) with the aug-cc-pVQZ basis set are shown in *SI Appendix*, Fig. S3. The curve calculated by revM06-L is closer to the CCSD(T) result than is the M06-L curve, especially in the region where the distance is longer than the equilibrium one, even though the training set has only one binding energy of the water dimer in the NCCE30 database. Therefore, we conclude that the revM06-L functional is more suitable than M06-L for molecular dynamics simulation involving water.

Conclusions

This work presents a revised version, called revM06-L, of the M06-L exchange–correlation functional for KS-DFT. The aim of this study was to reparameterize the M06-L functional form for better across-the-board accuracy and more computational stability for both chemistry and condensed-matter physics problems. We removed some large integral terms in the functional form because they demand a finer grid size and more SCF iterations, and then we optimized the revM06-L functional with smoothness restraints against Minnesota Database 2015A. As a result of the smoothness restraints, the parameters in revM06-L are much smaller than those in M06-L, and the number of parameters in revM06-L is reduced from 34 to 31; furthermore, the revM06-L functional gives smoother potential curves for rare gas dimers, with reduced grid errors and improved computational stability.

The overall performance of revM06-L on AME422 is improved over M06-L, with the MUE decreased from 3.6 kcal/mol to 3.1 kcal/mol. The performance of revM06-L for chemical reaction barrier heights (BH76), noncovalent interactions (NC51), and solid-state lattice constants (LC17) is especially significantly improved.

Because revM06-L and MN15-L are the two best-performing local functionals if judged by the overall MUE in Table 1, it is useful to compare them in more detail. For the 25 AME subdatabases in *SI Appendix*, Table S5, MN15-L has an MUE that is lower by more than 1% for 19 of them. For isomerization energies of large molecules and bond energies of multireference TM dimers, the two functionals have MUEs that agree within 1%, but revM06-L has a smaller MUE for the following four subdatabases: absolute atomic energies of atoms, bond energies of single-reference main-group metals, noncovalent complexation energies, and hydrocarbon chemistry (by, respectively, 36%, 29%, 25%, and 13%). The revM06-L functional also has a smaller MUE for diatomic geometries of heavy-atom molecules (by 36%), for solid-state lattice constants (by 11%), and for semiconductor band gaps (by 44%). Note that semiconductor band gaps were not included in the training set. The ultimate usefulness of the various functionals will likely only emerge, however, after they are applied to many more problems to see how well they withstand the test of time.

For the nontraining test sets, the revM06-L functional gives the best results among all local functionals for databases of semiconductor band gaps (SBG31), noncovalent interactions (S66), excitation energies (EE69), transition-metal coordination reactions (WCCR10), and alkyl bond dissociation energies (ABDE13). In addition, revM06-L gives the second-best results (behind MN15-L) among local functionals for TM reaction barrier heights (TMBH21). For WCCR10, revM06-L even performs better than all hybrid functionals tested in this work and previous studies by us and other researchers.

Local functionals are computationally efficient for solid-state systems with plane wave basis sets, and therefore revM06-L is especially suitable for practical computations on simulations of condensed-phase systems.

We conclude that the revM06-L functional is well suited for a broad range of applications in chemistry and condensed-matter physics.

ACKNOWLEDGMENTS. We thank Pragya Verma for helpful assistance. This work was supported by the National Natural Science Foundation of China (Grants 21303057 and 21673074), Ministry of Science and Technology of China (Grant 2016YFA0501700), Specialized Research Fund for the Doctoral Program of Higher Education (Grant 20130076120019), Youth Top-Notch Talent Support Program of Shanghai, New York University–East China Normal University (NYU–ECNU) Center for Computational Chemistry at NYU Shanghai, and US Department of Energy, Basic Energy Sciences (Award DE-SC0012702 to the Inorganometallic Catalysis Design Center).

1. Cohen AJ, Mori-Sánchez P, Yang W (2012) Challenges for density functional theory. *Chem Rev* 112:289–320.
2. Yang W, Cohen AJ, Mori-Sánchez P (2012) Derivative discontinuity, bandgap and lowest unoccupied molecular orbital in density functional theory. *J Chem Phys* 136:204111.
3. Becke AD (1992) Density-functional thermochemistry. I. The effect of the exchange-only gradient correction. *J Chem Phys* 96:2155–2160.
4. Ernzerhof M, Burke K, Perdew JP (1996) Long-range asymptotic behavior of ground-state wave functions, one-matrices, and pair densities. *J Chem Phys* 105:2798–2803.
5. Adamo C, Barone V (1998) Exchange functionals with improved long-range behavior and adiabatic connection methods without adjustable parameters: The mPW and mPW1PW models. *J Chem Phys* 108:664–675.
6. Zhao Y, Schultz NE, Truhlar DG (2006) Design of density functionals by combining the method of constraint satisfaction with parametrization for thermochemistry, thermochemical kinetics, and noncovalent interactions. *J Chem Theory Comput* 2: 364–382.
7. Dunlap BI, Connolly JWD, Sabin JR (1979) On first-row diatomic molecules and local density models. *J Chem Phys* 71:4993–4999.
8. Vahtras O, Almlöf J, Feyereisen MW (1993) Integral approximations for LCAO-SCF calculations. *Chem Phys Lett* 213:514–518.
9. Jung Y, Sodt A, Gill PMW, Head-Gordon M (2005) Auxiliary basis expansions for large-scale electronic structure calculations. *Proc Natl Acad Sci USA* 102:6692–6697.
10. Eichkorn K, Treutler O, Öhm H, Häser M, Ahlrichs R (1995) Auxiliary basis sets to approximate Coulomb potentials. *Chem Phys* 240:283–290.
11. Eichkorn K, Weigend F, Treutler O, Ahlrichs R (1997) Auxiliary basis sets for main row atoms and transition metals and their use to approximate Coulomb potentials. *Theor Chem Acc* 97:119–124.
12. Baerends EJ, Ellis DE, Ros P (1973) Self-consistent molecular Hartre-Fock-Slater calculations I. The computational procedure. *Chem Phys* 2:41–51.
13. Kohn W (1999) Nobel Lecture: Electronic structure of matter-wave functions and density functionals. *Rev Mod Phys* 71:1253–1266.
14. Zhao Y, Truhlar DG (2008) The M06 suite of density functionals for main group thermochemistry, thermochemical kinetics, noncovalent interactions, excited states, and transition elements: Two new functionals and systematic testing of four M06-class functionals and 12 other functionals. *Theor Chem Acc* 120:215–241.
15. Schultz NE, Zhao Y, Truhlar DG (2005) Density functionals for inorganometallic and organometallic chemistry. *J Phys Chem A* 109:11127–11143.
16. Schultz NE, Zhao Y, Truhlar DG (2005) Databases for transition element bonding: Metal-metal bond energies and bond lengths and their use to test hybrid, hybrid meta, and meta density functionals and generalized gradient approximations. *J Phys Chem A* 109:4388–4403.
17. Yu HS, He X, Truhlar DG (2016) MN15-L: A new local exchange-correlation functional for Kohn–Sham density functional theory with broad accuracy for atoms, molecules, and solids. *J Chem Theory Comput* 12:1280–1293.
18. Yu HS, He X, Li SL, Truhlar DG (2016) MN15: A Kohn–Sham global-hybrid exchange–correlation density functional with broad accuracy for multi-reference and single-reference systems and noncovalent interactions. *Chem Sci (Camb)* 7:5032–5051.
19. Zhao Y, Truhlar DG (2006) A new local density functional for main-group thermochemistry, transition metal bonding, thermochemical kinetics, and noncovalent interactions. *J Chem Phys* 125:194101.
20. Peverati R, Truhlar DG (2011) M11-L: A local density functional that provides improved accuracy for electronic structure calculations in chemistry and physics. *J Phys Chem Lett* 3:117–124.
21. Peverati R, Truhlar DG (2012) An improved and broadly accurate local approximation to the exchange-correlation density functional: The MN12-L functional for electronic structure calculations in chemistry and physics. *Phys Chem Chem Phys* 14:13171–13174.
22. Sun J, et al. (2013) Density functionals that recognize covalent, metallic, and weak bonds. *Phys Rev Lett* 111:106401.
23. Wheeler SE, Houk KN (2010) Integration grid errors for meta-GGA-predicted reaction energies: Origin of grid errors for the M06 suite of functionals. *J Chem Theory Comput* 6:395–404.
24. Perdew JP, Ruzsinszky A, Csonka GI, Constantin LA, Sun J (2009) Workhorse semilocal density functional for condensed matter physics and quantum chemistry. *Phys Rev Lett* 103:026403.
25. Sun J, et al. (2013) Semilocal and hybrid meta-generalized gradient approximations based on the understanding of the kinetic-energy-density dependence. *J Chem Phys* 138:044113.
26. Yu HS, Zhang W, Verma P, He X, Truhlar DG (2015) Nonseparable exchange-correlation functional for molecules, including homogeneous catalysis involving transition metals. *Phys Chem Chem Phys* 17:12146–12160.
27. Zhao Y, et al. (2017) *MN-GFM, Version 6.8: Minnesota Gaussian Functional Module* (Univ Minnesota, Minneapolis).
28. Frisch MJ, et al. (2009) *Gaussian 09, Revision C.01* (Gaussian, Inc., Wallingford, CT).
29. Hamprecht FA, Cohen AJ, Tozer DJ, Handy NC (1998) Development and assessment of new exchange-correlation functionals. *J Chem Phys* 109:6264–6271.
30. Perdew JP, Burke K, Ernzerhof M (1996) Generalized gradient approximation made simple. *Phys Rev Lett* 77:3865–3868.
31. Tao J, Perdew JP, Staroverov VN, Scuseria GE (2003) Climbing the density functional ladder: nonempirical meta-generalized gradient approximation designed for molecules and solids. *Phys Rev Lett* 91:146401.
32. Becke AD (1988) Density-functional exchange-energy approximation with correct asymptotic behavior. *Phys Rev A Gen Phys* 38:3098–3100.
33. Lee C, Yang W, Parr RG (1988) Development of the Colle-Salvetti correlation-energy formula into a functional of the electron density. *Phys Rev B Condens Matter* 37: 785–789.
34. Stephens PJ, Devlin FJ, Chabalowski CF, Frisch MJ (1994) Ab-initio calculation of vibrational absorption and circular-dichroism spectra using density-functional force-fields. *J Phys Chem* 98:11623–11627.
35. Van Voorhis T, Scuseria GE (1998) A novel form for the exchange-correlation energy functional. *J Chem Phys* 109:400–410.
36. Boese AD, Handy NC (2002) New exchange-correlation density functionals: The role of the kinetic-energy density. *J Chem Phys* 116:9559–9569.
37. Chai JD, Head-Gordon M (2008) Long-range corrected hybrid density functionals with damped atom-atom dispersion corrections. *Phys Chem Chem Phys* 10:6615–6620.
38. Zhao Y, Truhlar DG (2008) Exploring the limit of accuracy of the global hybrid meta density functional for main-group thermochemistry, kinetics, and noncovalent interactions. *J Chem Theory Comput* 4:1849–1868.
39. Klimeš J, Michaelides A (2012) Perspective: Advances and challenges in treating van der Waals dispersion forces in density functional theory. *J Chem Phys* 137:120901.
40. Dion M, Rydberg H, Schröder E, Langreth DC, Lundqvist BI (2004) van der Waals density functional for general geometries. *Phys Rev Lett* 92:246401.
41. Vydrov OA, Van Voorhis T (2010) Nonlocal van der Waals density functional: The simpler the better. *J Chem Phys* 133:244103.
42. Grimme S, Antony J, Ehrlich S, Krieg H (2010) A consistent and accurate ab initio parametrization of density functional dispersion correction (DFT-D) for the 94 elements H-Pu. *J Chem Phys* 132:154104.
43. Krukau AV, Vydrov OA, Izmaylov AF, Scuseria GE (2006) Influence of the exchange screening parameter on the performance of screened hybrid functionals. *J Chem Phys* 125:224106.
44. Posada-Borbón A, Posada-Amarillas A (2014) Theoretical DFT study of homonuclear and binary transition-metal dimers. *Chem Phys Lett* 618:66–71.
45. Rezáč J, Riley KE, Hobza P (2011) S66: A well-balanced database of benchmark interaction energies relevant to biomolecular structures. *J Chem Theory Comput* 7: 2427–2438.
46. Goerigk L, Kruse H, Grimme S (2011) Benchmarking density functional methods against the S66 and S66x8 datasets for non-covalent interactions. *ChemPhysChem* 12: 3421–3433.
47. Zhao Y, Truhlar DG (2005) Design of density functionals that are broadly accurate for thermochemistry, thermochemical kinetics, and nonbonded interactions. *J Phys Chem A* 109:5656–5667.
48. Grimme S, Ehrlich S, Goerigk L (2011) Effect of the damping function in dispersion corrected density functional theory. *J Comput Chem* 32:1456–1465.
49. Leverentz HR, Siepmann JI, Truhlar DG, Loukonen V, Vehkamäki H (2013) Energetics of atmospherically implicated clusters made of sulfuric acid, ammonia, and dimethyl amine. *J Phys Chem A* 117:3819–3825.
50. Isegawa M, Peverati R, Truhlar DG (2012) Performance of recent and high-performance approximate density functionals for time-dependent density functional theory calculations of valence and Rydberg electronic transition energies. *J Chem Phys* 137:244104.
51. Caricato M, Trucks GW, Frisch MJ, Wiberg KB (2010) Electronic transition energies: A study of the performance of a large range of single reference density functional and wave function methods on valence and Rydberg states compared to experiment. *J Chem Theory Comput* 6:370–383.
52. Adamo C, Barone V (1999) Toward reliable density functional methods without adjustable parameters: The PBE0 model. *J Chem Phys* 110:6158–6170.
53. Chai JD, Head-Gordon M (2008) Systematic optimization of long-range corrected hybrid density functionals. *J Chem Phys* 128:084106.
54. Weymuth T, Couzijn EP, Chen P, Reiher M (2014) New benchmark set of transition-metal coordination reactions for the assessment of density functionals. *J Chem Theory Comput* 10:3092–3103.
55. Hu L, Chen H (2015) Assessment of DFT methods for computing activation energies of Mo/W-mediated reactions. *J Chem Theory Comput* 11:4601–4614.
56. Sun Y, Chen H (2013) Performance of density functionals for activation energies of Zr-mediated reactions. *J Chem Theory Comput* 9:4735–4743.
57. Sun Y, Chen H (2014) Performance of density functionals for activation energies of Re-catalyzed organic reactions. *J Chem Theory Comput* 10:579–588.
58. Tishchenko O, Zheng J, Truhlar DG (2008) Multireference model chemistries for thermochemical kinetics. *J Chem Theory Comput* 4:1208–1219.
59. Xu X, Alecu IM, Truhlar DG (2011) How well can modern density functionals predict internuclear distances at transition states? *J Chem Theory Comput* 7:1667–1676.
60. Tang KT, Toennies JP (2003) The van der Waals potentials between all the rare gas atoms from He to Rn. *J Chem Phys* 118:4976–4983.